

Low threshold, high temperature operation of continuous wave interband cascade lasers near 5 μm

Yuzhe Lin,^{1, a)} Yuan Ma,¹ Wanhua Zheng^{1, a)}, Kedong Zhang,² Hong Lu,² and Rui Q. Yang³

¹*Laboratory of Solid State Optoelectronics Information Technology, Institute of Semiconductors, Chinese Academy of Sciences, Beijing 100083, China*

²*National Laboratory of Solid State Microstructures & Department of Materials Science and Engineering, College of Engineering and Applied Sciences, Nanjing University, Nanjing 210093, China*

³*School of Electrical and Computer Engineering, University of Oklahoma, Norman, OK 73019, USA*

^{a)}*Author to whom correspondence should be addressed. Electronic mail:*
linyuzhe@semi.ac.cn; whzheng@semi.ac.cn.

Abstract

We report significant improvements in threshold current density and maximum operating temperature in continuous wave (CW) operation of interband cascade lasers (ICLs) near 5 μm . The uncoated ICLs were demonstrated at room temperature with a threshold current density of 343.8 A/cm² and an output power of 31 mW/facet at 25°C in CW mode. Different ICLs made from the same wafer were compared to study the impact of device dimensions on performance. The threshold current density of 331 A/cm² achieved from a facet-uncoated 5 mm-long device at 25°C is the lowest among all previously reported room temperature CW ICLs with emission wavelengths longer than 4 μm . Compared to the previous record of 480 A/cm² at 4.75 μm for a facet-coated 4-mm-long ICL at 25°C, this value of 331 A/cm² is reduced by 31%, representing a substantial improvement. Benefited from improved device fabrication and enhanced thermal dissipation, the maximum CW operating temperature of the device reached 66 °C, which is the highest ever reported for ICLs with similar emission wavelengths.

Keywords: interband cascade; quantum well; semiconductor lasers; mid-infrared; thermal dissipation.

After about 30 years of development since the proposal of the initial concept [1], interband cascade laser (ICL) has become a major mid-infrared semiconductor laser technology with a vast potential for many applications [2-4]. By combining advantages of interband transitions of diode lasers and the cascade configuration of quantum cascade lasers [5], ICLs based on type-II quantum well (QW) active region are able to operate with low power consumption and cover a wide wavelength range from 2.7 μm to beyond 14 μm [2-4, 6-12]. In the 3-4 μm wavelength region, ICLs achieved very efficient continuous wave (CW) operation at room temperature (RT) with threshold current density (J_{th}) as low as 156 A/cm² [12]. However, at wavelengths longer than 4 μm , their CW RT threshold current densities were typically more than 500 mA/cm² [2-3, 7-8, 13-19] and the lowest reported J_{th} was 480 A/cm² at 4.75 μm for a facet-coated 4-mm-long ICL at 25°C [13], although the pulsed RT J_{th} of their corresponding broad-area (BA) ICLs could be below 300 A/cm² (e.g. 220 A/cm² [15] and 252 A/cm² [16]). This was due mainly to the combination of relatively poor thermal dissipation and sidewall effect that caused a substantial leakage current and optical scattering loss. The sidewall effect becomes more significant when the ridge of an ICL device is narrower and the lasing wavelength is longer with a smaller bandgap. Also, thermal dissipation becomes poorer at longer wavelengths because of the thicker cladding layers, which is especially severe in the case of InAs/AlSb short-period superlattice (SL) cladding. The issues due to the SL cladding have been addressed by a waveguide approach using hybrid cladding layers [14]. This approach is very effective particularly for ICLs on InAs substrates at long wavelengths [3], which dramatically reduces the SL cladding thickness and helps the device thermal dissipation.

In this work, by applying an epi-side down mounting technique to InAs-based ICLs with hybrid cladding layers, thermal dissipation is further enhanced. In addition, the sidewall effect is reduced when the narrow ridge (NR) device fabrication is improved using an inductively coupled plasma (ICP) dry etching approach. As such, the fabricated NR ICL devices achieved CW operation at temperatures up to 66°C at a wavelength near 5.1 μm , representing the highest CW operating temperature among ICLs with similar lasing wavelengths. More importantly, threshold current density as low as 331 A/cm² was achieved at RT (25°C), which is substantially lower than any values of RT CW J_{th} among ICLs at wavelengths longer than 4 μm .

A piece of ICL wafer B that was described in Ref. 16 was fabricated to NR devices with ridge widths of 7, 10, 20 and 30 μm using an inductively coupled plasma (ICP) etching containing gas mixtures of methane and hydrogen. A 200-nm-thick Si₃N₄ and 200-nm-thick SiO₂ layers were deposited by plasma-enhanced chemical vapor deposition for insulation. Ti/Au metals were applied for the top contact with a 6 μm -thick Au layer deposited by electroplating. After substrate was thinned down to about 120 μm , an AuGeNi/Au metal contact was deposited on the backside of the substrate. The ICL structure was grown on a undoped n-type InAs substrate (carrier concentration: 1-3×10¹⁶/cm³) by a Veeco GENxplor MBE system, which has 10 cascade stages and hybrid cladding layers consisting of InAs/AlSb SLs and heavily-doped n-type InAs. BA devices made previously from this wafer could lase in a pulsed mode near 4.84 μm at 300 K with a J_{th} as low as 269 A/cm² (for a cavity length L of 1.5 mm). More structural details were given in Ref. [16]. The fabricated NR devices were cleaved into 2-mm, 3-mm and 5-mm-long laser devices without facet coating. They were mounted epi-side down on diamond submounts using indium solder for testing. A Fourier transform infrared spectrometer was used to record the lasing spectra.

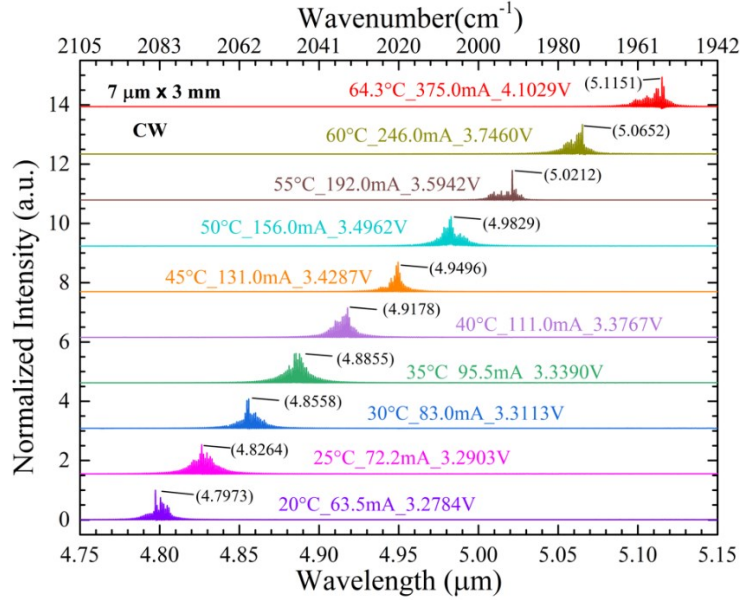


FIG. 1. CW lasing spectra for a $7 \mu\text{m} \times 3 \text{ mm}$ ICL at various temperatures.

A $7 \mu\text{m} \times 3 \text{ mm}$ ICL lased in CW mode at temperatures up to 64.3°C with a lasing wavelength near $5.12 \mu\text{m}$ shifted from $4.80 \mu\text{m}$ at 20°C as shown in Fig. 1. The wavelength shift with temperature was at an initial rate of 5.8 nm/K from 20°C and increased at higher temperatures especially when it was closer to the maximum CW operating temperature of 64.3°C . The CW wavelength shifting rate with temperature is higher than pulsed lasing wavelength shifting rate of 4.8 nm/K obtained from a BA device near 300 K , indicating apparent heating generated in CW operation, which became more significant at higher temperatures. Its maximum CW operating temperature of 64.3°C is about the same as that of a facet-coated epi-side down mounted 2-mm-long ICL with a somewhat shorter wavelength near $4.8 \mu\text{m}$ at 64°C reported in Ref. 17 and 23 K higher than that of a facet-coated epi-side down mounted 2-mm-long ICL with a slightly longer wavelength near $5.28 \mu\text{m}$ at 41°C reported in Ref. 18. The higher CW operating temperature achieved can be attributed to the enhanced thermal dissipation with the epi-side down mounting on a diamond submount and reduced threshold current density. The enhanced thermal dissipation also helped to reduce the CW threshold current density and improve wall-plug efficiency (WPE). For example, at 25°C , its CW threshold current density was 343.8 A/cm^2 , much lower than the best value of RT CW J_{th} ever reported for either GaSb-based or InAs-based ICLs at wavelengths longer than $4 \mu\text{m}$. Its threshold voltage (V_{th}) at 25°C was 3.29 V , corresponding to a threshold power density (P_{th}) of 1.13 kW/cm^2 and a voltage efficiency of 78% that is also the highest among RT CW ICLs. Consequently, appreciable CW output power was obtained from this ICL device as shown in Fig. 2 by its current-voltage-light (IVL) characteristics at various temperatures. At 25°C , the measured single facet output power reached 31 mW with an input current of 350 mA and was not saturated yet. It could deliver a higher output power with a larger current. We did not operate it with larger currents to avoid accidental damage. Nevertheless, the total output power from both facets was already substantially higher than the best value reported previously for ICLs at similar wavelengths. The WPE reached a maximum value of 4.64% at 220 mA at 25°C , which is appreciable at such a long wavelength for a relatively low power device. Its WPE decreased gradually with larger currents or at high temperatures due to more heating generated as shown in

Fig. 2. However, even at 60 °C, the device could still have a WPE of 0.37% with a CW output power of exceeding 2 mW/facet, sufficient for some sensing applications.

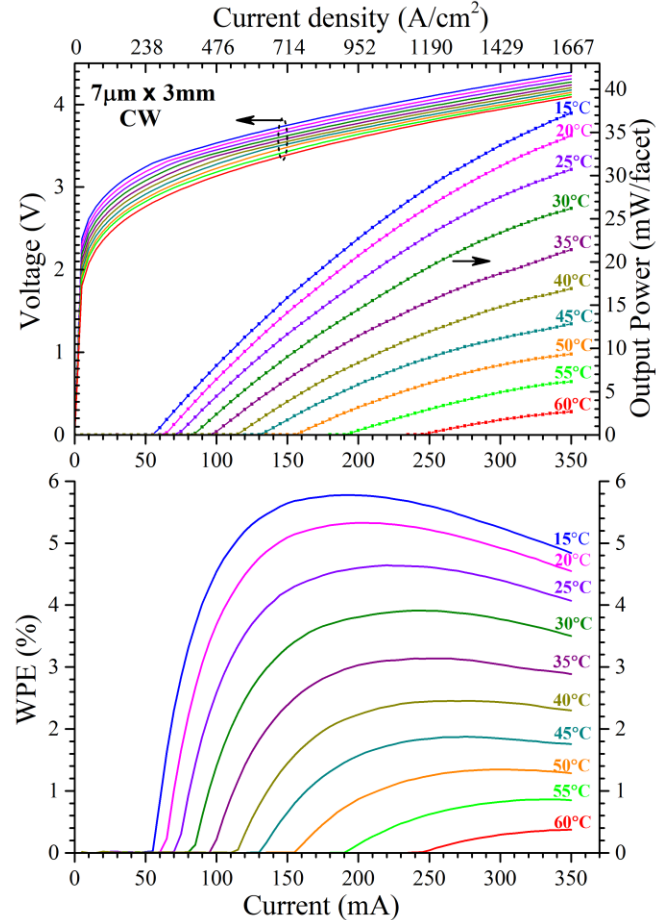


FIG. 2. IVL characteristics (the top panel) and WPE (the bottom panel) for a 7 $\mu\text{m} \times 3$ mm uncoated ICL with epi-side down on a diamond submount at a temperature range from 15 °C to 60 °C operating in CW mode.

To evaluate the device performance on NR ICL dimensions, ICLs with different ridge widths and cavity lengths were investigated and their CW threshold current densities are plotted in Fig. 3 as a function of temperature together with the pulsed threshold current density of a representative BA device that was mounted epi-side up on a Cu heat sink. At 25°C, the J_{th} of a 7 $\mu\text{m} \times 2$ mm device is 17% higher than J_{th} of a 30 $\mu\text{m} \times 2$ mm ICL. This difference increased to 20% at 20°C even with a reduced heating effect shown in the 30 $\mu\text{m} \times 2$ mm ICL as it had the lowest CW threshold current density (285 A/cm²) at this temperature (20°C). This indicates the existence of a substantial sidewall effect, which increased J_{th} at least by 20% for the 7- μm -wide NR ridge devices compared to the wider devices. The 30- μm -wide NR device had the lowest sidewall effect (~12% extracted by comparing its CW J_{th} with the pulsed J_{th} of the BA device if the cavity length difference is ignored). However, the 30- μm -wide NR device had a stronger Joule heating with relatively high current and its J_{th} increased more rapidly with temperature, which limited its maximum CW operating temperature to 322 K (49°C) as shown in Fig. 3. By comparing J_{th} between the CW 7 $\mu\text{m} \times 2$ mm device and the pulsed BA device at 25°C, the increased percentage of J_{th} was ~41% for the 7- μm -wide device due to additional Joule heating. Hence, considering all the factors discussed

above, the sidewall effect increased J_{th} by a percentage between 32% and 41% for the 7- μm -wide device. This is substantially lower than the 45%-71% [14] (and close to 100% [17-18]) difference in InAs-based ICLs in the wavelength range of 4.6 to 5.2 μm , but higher than the ~21% for the best fabricated NR GaSb-based ICLs in the 3-4 μm wavelength region [20]. This comparison suggests substantially improved NR device fabrication obtained in this study and there is still room for further development.

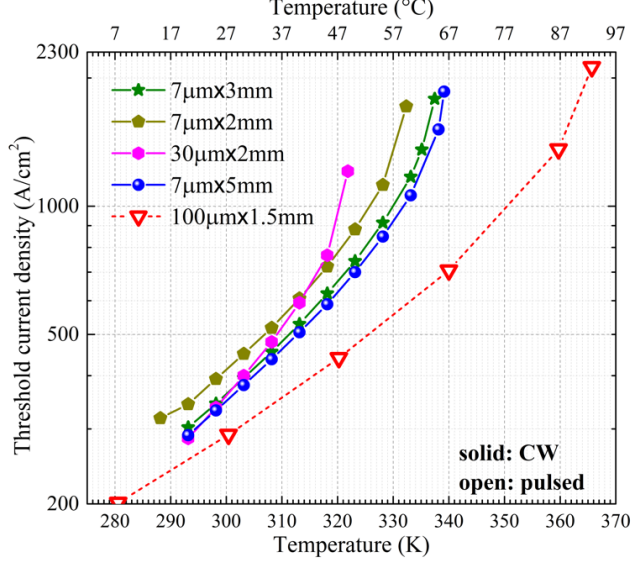


FIG. 3. Temperature dependent threshold current density of ICL devices in both CW and pulsed modes with different device sizes and packaging.

With increased cavity length, the mirror loss is reduced and thus the threshold current density could be lowered. As shown in Fig. 3, the 7 $\mu\text{m} \times 3$ mm device had J_{th} reduced to 344 A/cm^2 compared to 393 A/cm^2 for a 2-mm-long ICL at 25°C, which raised the maximum CW operating from 332 K (59°C) to 337 K (64°C). However, the longer cavity length requires a higher total current, which increases the Joule heating. The maximum WPE was higher (e.g. 5.91% at 160 mA at 25°C) for the 2-mm-long ICL. Hence, a further increment of the cavity from 3 mm to 5 mm gained less benefit and only slightly reduced the J_{th} (e.g. 331 A/cm^2 at 25°C). Nevertheless, it helped the device to lase in CW mode up to 66°C at a lasing wavelength near 5.1 μm as shown in the inset of Fig. 4,

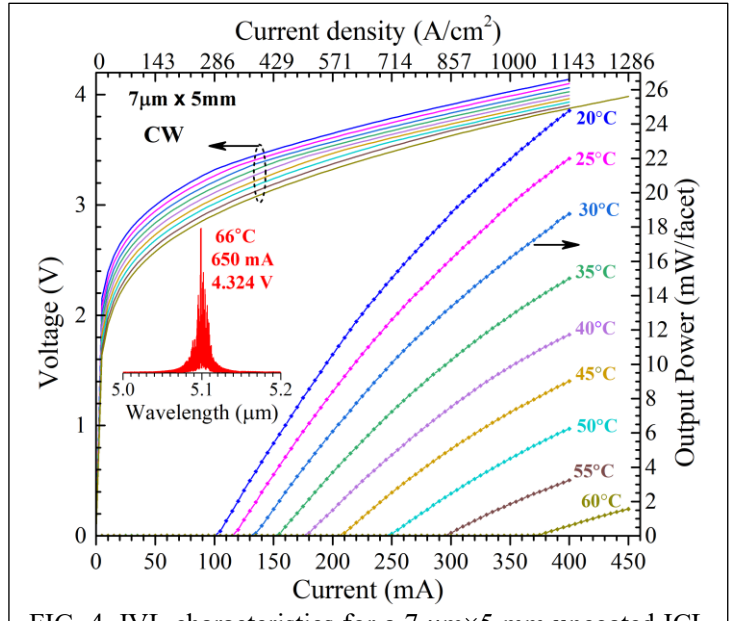


FIG. 4. IVL characteristics for a 7 $\mu\text{m} \times 5$ mm uncoated ICL with epi-side down on a diamond submount at a temperature range from 15 °C to 60 °C in CW mode. The inset is its CW lasing spectrum at 66°C.

the highest CW operating temperature for ICLs at similar wavelengths. Also, the threshold current density of 331 A/cm^2 is the lowest among RT CW semiconductor lasers at this wavelength, representing an obvious advancement. With the longer cavity, a larger current could be injected into the ICL device, possibly to achieve a higher output power. However, to avoid possible accidental damage, the injection current was limited to 450 mA except at 66°C . So, the output power was limited to 25 mW/facet as shown in Fig. 4 for its IVL characteristics. But the output power was far away from saturation at 400 or 450 mA as can be inspected from Fig. 4. Therefore, an output power exceeding 40 mW/facet at 20°C is viable with a higher current. Alternatively, to reduce threshold current density and increase output power at a lower current, applying facet coating to ICLs would be more effective, which will be explored in our future work.

In summary, applying epi-side down mounting and using ICP dry etching, NR InAs-based ICLs at emission wavelength near $5 \mu\text{m}$ were demonstrated in CW operation at RT and above. The RT CW threshold current density of 331 A/cm^2 is the lowest ever achieved among RT CW semiconductor lasers at similar wavelengths. The maximum CW operating temperature of 66°C is also the highest ever demonstrated for ICLs at this wavelength. Our analysis on ICLs with different dimensions suggests more room available for further advancement.

ACKNOWLEDGMENTS

This work at Institute of Semiconductors, Chinese Academy of Sciences was supported in part by the National Natural Science Foundation of China under Grants No. 12393833, the work at Nanjing University was partially supported by the National Key Research and Development Program of China under Grant No. 2023YFA1406903, the work at the University of Oklahoma was partially supported by NSF (No. ECCS-1931193). The authors thank Y. Y. Zhang, H. Li and Y. Z. Huang for helpful discussion on the Sb-based devices fabrication process.

Data Availability Statement

The data that support the findings of this study are available from the corresponding author upon reasonable request.

REFERENCES

- [1] R. Q. Yang, "Infrared laser based on intersubband transitions in quantum wells," at 7th Inter. Conf. on Superlattices, *Microstructures and Microdevices*, Banff, Canada, August, 1994; *Superlattices and Microstructures*, **17**, 77 (1995).
- [2] J. R. Meyer, W. W. Bewley, C. L. Canedy, C. S. Kim, M. Kim, C. D. Merritt, and I. Vurgaftman, "The Interband Cascade Laser," *Photonics*, **7**, 75 (2020).
- [3] R. Q. Yang, L. Li, W. Huang, S. M. Rassel, J. A. Gupta, A. Bezinger, X. Wu, S. G. Razavipour, and G. C. Aers, "InAs-Based Interband Cascade Lasers," *IEEE Journal of Selected Topics in Quantum Electronics*, **25**, 1200108 (2019).
- [4] I. Vurgaftman, R. Weih, M. Kamp, J. R. Meyer, C. L. Canedy, C. S. Kim, M. Kim, W. W. Bewley, C. D. Merritt, J. Abell, and S. Hofling, "Interband cascade lasers," *Journal of Physics D-Applied Physics*, Article vol. **48**, 123001 (2015).
- [5] J. Faist, F. Capasso, D. L. Sivco, C. Sirtori, A. L. Hutchinson, and A. Y. Cho, "Quantum cascade laser," *Science*, **264**, 553 (1994).

[6] I. Vurgaftman, W. W. Bewley, C. L. Canedy, C. S. Kim, M. Kim, C. D. Merritt, J. Abell, J. R. Lindle, and J. R. Meyer, "Rebalancing of internally generated carriers for mid-infrared interband cascade lasers with very low power consumption," *Nature Communications*, **2**, 585 (2011).

[7] H. Knotig, J. Nauschütz, N. Opacak, S. Hofling, J. Koeth, R. Weih, and B. Schwarz, "Mitigating valence intersubband absorption in interband cascade lasers," *Laser & Photonics Reviews*, **16**, 2200156 (2022).

[8] J. Nauschütz, H. Knotig, R. Weih, J. Scheuermann, J. Koeth, S. Hofling, and B. Schwarz, "Pushing the Room Temperature Continuous-Wave Operation Limit of GaSb-Based Interband Cascade Lasers beyond 6 μm ," *Laser & Photonics Reviews*, **17**, 2200587 (2023).

[9] J. A. Massengale, Y. X. Shen, R. Q. Yang, S. D. Hawkins, and A. J. Muhowski, "Low Threshold, Long Wavelength Interband Cascade Lasers With High Voltage Efficiencies," *IEEE Journal of Quantum Electronics*, **59**, 200050 (2023).

[10] Y. Shen, R. Q. Yang, S. D. Hawkins, and A. J. Muhowski, "Continuous wave interband cascade lasers near 13 μm ," *Journal of Vacuum Science & Technology B*, **42**, 022206 (2024).

[11] Y. Shen, J. A. Massengale, R. Q. Yang, S. D. Hawkins, and A. J. Muhowski, "Pushing the performance limits of long wavelength interband cascade lasers using innovative quantum well active regions," *Applied Physics Letters*, **123**, 041108 (2023).

[12] W. W. Bewley, C. L. Canedy, C. S. Kim, M. Kim, C. D. Merritt, J. Abell, I. Vurgaftman, and J. R. Meyer, "High-power room-temperature continuous-wave mid-infrared interband cascade lasers," *Optics Express*, **20**, 20894 (2012).

[13] W. W. Bewley, C. L. Canedy, C. S. Kim, M. Kim, C. D. Merritt, J. Abell, I. Vurgaftman, and J. R. Meyer, "Continuous-wave interband cascade lasers operating above room temperature at $\lambda = 4.7\text{-}5.6 \mu\text{m}$," *Optics Express*, **20**, 3235 (2012).

[14] L. Li, Y. C. Jiang, H. Ye, R. Q. Yang, T. D. Mishima, M. B. Santos, and M. B. Johnson, "Low-threshold InAs-based interband cascade lasers operating at high temperatures," *Applied Physics Letters*, **106**, 251102 (2015).

[15] C. Canedy, M. Warren, C. Merritt, W. Bewley, C. Kim, M. Kim, I. Vurgaftman, and J. R. Meyer, "Interband cascade lasers with longer wavelengths," Proc. *SPIE* **10111**, 101110G (2017).

[16] K. Zhang, Y. Lin, W. Zheng, R. Q. Yang, H. Lu, and Y. F. Chen, "Low threshold InAs-based interband cascade lasers grown by MBE," *Journal of Crystal Growth*, **586**, 126618 (2022).

[17] W. Huang, S. Hu, J. Tu, L. Zhang, K. Tao, and P. Wang, "High-temperature continuous-wave operation of InAs-based interband cascade laser," *Applied Physics Letters*, **123**, 151111 (2023).

[18] W. Huang, S. Hu, J. Tu, L. Zhang, K. Tao, and P. Wang, "InAs-Based Interband Cascade Laser Operating at 5.17 μm in Continuous Wave Above Room Temperature," *IEEE Photonics Technology Letters*, **36**, 91 (2024).

[19] B. Petrović, A. Bader, J. Nauschütz, T. Sato, S. Birner, R. Weih, F. Hartmann, and S. Höfling, "GaSb-based interband cascade laser with hybrid superlattice plasmon-enhanced claddings," *Applied Physics Letters*, **124**, 241101 (2024).

[20] W. W. Bewley, C. L. Canedy, C. S. Kim, M. Kim, J. R. Lindle, J. Abell, I. Vurgaftman, and J. R. Meyer, "Ridge-width dependence of midinfrared interband cascade laser characteristics," *Optical Engineering*, **49**, article 111116 (2010).